

Received August 13, 2020; reviewed; accepted October 13, 2020

Thermodynamic analysis of the influence of potassium on the thermal behavior of kaolin raw material

Macaria Hernández-Chávez^{1,2}, Marissa Vargas-Ramírez¹, Ana M. Herrera-González¹,
Jesús García-Serrano¹, Alejandro Cruz-Ramírez³, José A. Romero-Serrano⁴,
Ricardo G. Sánchez-Alvarado⁴

¹ Instituto de Ciencias Básicas e Ingeniería, Universidad Autónoma del Estado de Hidalgo (UAEH), México

² Laboratorio de Química, UPIIH, Instituto Politécnico Nacional, Ciudad del Conocimiento y la Cultura, San Agustín Tlaxiaca, Hidalgo, 42162, México

³ Departamento de Formación Básica Disciplinaria. Instituto Politécnico Nacional – Unidad Profesional Interdisciplinaria de Ingeniería campus Hidalgo (UPIIH-IPN), México

⁴ Departamento de Ingeniería en Metalurgia y Materiales. Instituto Politécnico Nacional – Escuela Superior de Ingeniería Química e Industrias Extractivas (ESIQIE-IPN), México

Corresponding author: alcruzr@ipn.mx (A. Cruz-Ramírez)

Abstract: The mineralogy and thermal properties of two kaolin clay samples from Agua Blanca (Hidalgo-México) were determined by XRD, SEM-EDS, TGA-DSC techniques. Kaolin clay A contains a higher Al_2O_3 and lower impurities (K_2O , TiO_2 , Fe_2O_3) amount than kaolin clay B, while the SiO_2 amount is similar for both kaolin clays. A theoretical approach was carried out by a thermodynamic analysis considering the chemical composition of both kaolin clay samples with the FactSage 7.3 software. Stability phase diagrams were obtained to different K_2O content from 0.1 to 3 wt % and temperatures in the range from 600 to 1600°C based on the chemical composition of the kaolin clay samples. The main mineralogical compounds predicted are andalusite ($\text{Al}_2\text{O}_3\cdot\text{SiO}_2$), K-Potash feldspar ($\text{K}_2\text{O}\cdot\text{Al}_2\text{O}_3\cdot 6\text{SiO}_2$), and the SiO_2 polymorphs (quartz, tridymite, and cristobalite) with small amounts of ferric-pseudobrookite ($\text{Fe}_2\text{O}_5\text{Ti}$), and rutile (TiO_2). As K_2O content is increased, the amounts of mullite and tridymite decrease meanwhile the potash feldspar is increased at high temperatures. A liquid phase is formed at around 1350 and 1400°C for the kaolin clay samples A and B, respectively. The viscosity of the melt is increased for the evaluated K_2O additions to 1400, 1500, and 1600°C.

Keywords: kaolin, thermal treatment, thermodynamic analysis, viscosity

1. Introduction

Clay minerals are one of the most important materials since they form the basis of pottery and building bricks. The properties of clays minerals are determined by the fact that they are layer materials which belong to a subgroup of the layer silicates (Carter and Norton, 2013). Clay minerals technology is growing immensely to produce various types of ceramic materials for having certain valuable properties from various aluminosilicate raw materials (Chakraborty, 2014). In general, the clay minerals included in kaolins are hydrated aluminum silicates rich mainly in kaolinite [$\text{Al}_2\text{Si}_2\text{O}_5(\text{OH})_4$] which include its polymorphic modifications (dickite and nacrite) (Carter and Norton, 2013; Kiseleva et al., 2011). Kaolinite, a clay mineral generally formed by the intense weathering or hydrothermal alteration of aluminosilicate minerals, such as feldspars and mica. As other mined minerals, kaolins contain many minerals, such as quartz, micas, and unaltered feldspars. They also contain minerals that act as pigments, including iron oxides or oxyhydroxides (lepidocrocite, goethite, and/ or hematite), which give a brown color, and the TiO_2 polymorphs anatase and/ or rutile, which gave a pink color (Zegeye et al., 2013). Kaolinite undergoes a dehydroxylation around 550°C, originating an amorphous material

called metakaolinite; as temperature increases around 900°C, a spinel-type phase is obtained which subsequently crystallizes into mullite and cristobalite amorphous compounds at temperatures from 1000 to 1100°C (Michot et al., 2008; Moreno-Tovar et al., 2014). Along with the firing of the kaolin raw material, there is a loss of porosity producing shrinkage. Mullite materials are suitable as refractories for steel, glass, and petrochemical industries, due to its high chemical stability, good thermal shock resistance, superior refractory properties, and its strength retained up to 1300°C (Michot et al., 2008; Moreno-Tovar et al., 2014; Schroeder et al., 2004). The presence of crystalline quartz in kaolin raw material reduces its plasticity in green, and shrinkage in firing and the aluminum oxide in composition increases refractoriness. The presence of Fe, Na, and K, as oxides, decreases the melting temperature also, acting as fusing agents while iron oxides act as powerful coloring agents (Schroeder et al., 2004). Kaolins which are relatively high in alkalis and/or iron will develop high shrinkage and low porosity at lower firing temperatures; kaolins which are relatively low in these fluxing elements will tend to be more refractory. The alkali and/or iron content will influence the rate at which melting will occur through their fluxing action on silica and alumina. Fine particle size will tend to increase the rate at which these reactions occur (Bloodworth et al., 1993). The compound transition sequence and the chemical composition during heating kaolinite are intensively affected in the presence of mineralizers. Generally speaking, K₂O, CaO, and MgO chemical components are related to minor constituents in kaolins. K₂O is a main component in the chemical system Si₂O-Al₂O₃-K₂O, and CaO and MgO can act as mineralizer in phase transformations to mullite. The addition of MgO to kaolinite caused mullite formation via spinel or γ -Al₂O₃ compound and that of CaO caused mullite formation directly from metakaolinite (Bulens and Delmon, 1977). S. Johnson et al (1982) determined the effect of adding K₂CO₃ to kaolinite, on its thermal behavior at high temperatures. It was found that K₂O accelerated the formation of mullite and cristobalite; however, A. Yamuna et al (2002) determined that mullite was crystallized only during kaolinite heating when K₂CO₃ was added as a mineralizer, and the crystallization of cristobalite was inhibited. A. Aras (2004) mixed kaolinite clays of different qualities with 20% of K-feldspar and determined the effect of heat treatment on the mineralogy of the fired products. The formation of mullite and cristobalite was observed in kaolinitic clay and the structure was dominated by the spiky primary mullite while the cristobalite formation was suppressed in illite/sericite rich clay bodies. The effect of different potassium salts (KNO₃, KF, K₂SO₄) on the formation of mullite from kaolinite was also evaluated (Li et al., 2009). The KF promotes the massive formation of mullite at 1100°C than KNO₃ and K₂SO₄. Because kaolin is often associated with variable quantities of muscovite mica, G. L. Lecomte et al (2007) evaluate the thermal transformation of kaolinite-muscovite mixtures up to 1000°C. They found an increase in the mullite crystallization and grain growth at 1050°C due to potassium diffusion ions from muscovite platelets into metakaolinite structure. In a further study, G. L. Lecomte et al (2011) investigate the densifying mechanisms during the sintering of kaolinite-muscovite mixtures by isothermal and non-isothermal methods. The kaolin densification proceeded by a viscous flux sintering, due to an amorphous phase and a diffusion mechanism at the grain boundaries. The K₂O was identified as one of the major components that inhibit the formation of cristobalite in kaolinite at 1250°C. They found that only crystallized mullite was formed when the K₂O content is higher than 1.99 wt. % (Li et al., 2009). Kaolin deposits are widely distributed in Mexico, usually located in the Trans-Mexican Volcanic Belt. Agua Blanca in Hidalgo and Huayacocotla in Veracruz are two economically important, well know kaolin deposits (De Pablo-Galán, 1978). M. Garcia et al (2015) determined the mineralogy and thermal properties of kaolin from Acoculco zone (Puebla-México) and compared them with kaolin clays from Agua Blanca and Huayacocotla zones. The Acoculco deposit is composed mainly of kaolinite and SiO₂ minerals, similar to those obtained in Huayacocotla and Agua Blanca but with a lower amount of alunite. The Acoculco kaolin presented a lower shrinkage than kaolins from Agua Blanca and Huayacocotla due to a lower alunite content. Based on the mineralogical and thermal properties of the kaolins evaluated, they concluded that the kaolins are suitable as a raw material for the ceramic industry. The knowledge of the mineralogical compounds formed and the viscosity properties and how they evolved during the sintering process of kaolin is essential for optimum sintering to the ceramic industry. In the literature, there are few works reported (Li et al., 2009; G. L. Lecomte et al., 2007) on the formation of the mineralogical compounds during the kaolin firing containing K₂O as an impurity as well as the rheological properties of the melt. The mineralogical

background of the kaolin clay from the Agua Blanca zone indicates that the source of K_2O is the alunite mineral and it is considered as a suitable material for the ceramic industry; thus, it's important to know the K_2O effect on the mullite formation for ceramic applications. The aim of this work it's to carry out a mineralogical and thermal characterization of two kaolinitic clays from the Agua Blanca zone by XRD, SEM-EDS, and TGA-DSC techniques. Based on the chemical composition of both kaolin clays, a thermodynamic analysis was carried out with the thermodynamic software FactSage 7.3 to determine the effect of increasing the K_2O content and the temperature on the mineralogical compounds formation as well as the viscosity determination of the melt to 1400, 1500, and 1600°C.

2. Materials and methods

For this study, about twenty large samples (20 to 30 kg each) were collected from the deposit of two mines in the Agua Blanca zone by selective sampling on the kaolin clay footprints by digging a pit or using a hand auger. The raw material was milled and air classified to remove grit and dried to reduce moisture. Afterward, the large samples were quartered to obtain a representative sample of around 1 kg for laboratory assessment. The two kaolin clay samples obtained from the Agua Blanca zone were characterized through the determination of mineralogical and chemical composition, particle size distribution, the morphology of the particles, and thermal analysis (TGA-DSC). These kaolin clay deposits were formed by hydrothermal alteration related to the volcanic activity of the Trans-Mexican Volcanic Belt (De Pablo-Galán, 1978).

The chemical composition was analyzed using plasma emission spectrophotometry (ICP-OES, model Optima 8300 by Perkin Elmer). The kaolin clay samples were digested in hydrofluoric acid (HF) and then neutralized in boric acid (H_3BO_3) according to the procedure reported by P. J. Potts (2003).

The particle size distribution of the kaolin clay samples was determined using a laser diffraction particle size analyzer. In this study, 2 mL of kaolin clay suspension (100 g/L) was added to 100 mL of deionized water and incubated in a water bath shaker at 30°C and 150 rpm. After the incubation, the samples were analyzed by a Beckman Coulter, model LS13320, equipped with a light scattering detector to measure the particle size distribution of the kaolin clay particles. All the measurements were carried out at room temperature. Three measurements were carried out for each sample and average values were reported.

The mineralogy of the kaolin raw materials was identified by X-ray powder diffraction measurements using an X-Ray Bruker D8 Focus with monochromatic $Cu K\alpha$ ($\lambda = 1.5418 \text{ \AA}$) radiation working in $\theta/2\theta$ configuration. Data were collected in an angular range from 10 to 70° with a step size of 0.02° and a counting time of 2°·min⁻¹. The kaolin clays quantification was performed by the Rietveld method using Bruker's TOPAS 4.2 software and the procedure reported by R. Cheary and A. Coelho (1992) for the raw material as received.

The size, morphology, and qualitative chemical analysis of the kaolin clay samples were determined with the scanning electron microscope Jeol 6300 and with energy dispersive spectra (SEM-EDS) analysis. An Au-Pd film was deposited on the surface of the powders to make them conductive. Images were obtained to different magnifications with backscattering electrons with 15 kV and 10 A.

Thermal analyses of the kaolin clay samples were studied by simultaneous differential scanning calorimetry and thermogravimetric analysis by using a TA Instruments SDT Q600 simultaneous TGA-DSC. A heating rate of 10°C·min⁻¹ was used with an airflow rate of 50 ml min⁻¹ in alumina crucibles. Data were collected for a temperature range from 25 to 1200°C.

1 g of the kaolin clay samples were heated in the range from 500 to 1100°C. The thermal treatment was carried out in an electric kiln with a heating rate of 10°C·min⁻¹ and a soaking time of 1 h, and air-cooled. After thermal treatment, all the calcined samples were tested to determine the crystalline phase by X-ray powder diffraction test. The calcined sample to 1100°C was quantified by the Rietveld Method.

2.1. Thermodynamic Modeling

FactSage 7.3 (Bale et al., 2002) with the module Equilib was used to determine the concentration of the different chemical species once they reach the chemical equilibrium state. The user gives the initial amount of chemical species contained in the kaolin clay samples, the temperature and the pressure of the system (usually 1 atm), then the program calculates the most stable species with the Gibbs free

energy minimization method. The computer simulation was carried out using the FactPS and the FToxid databases. It is worth to mention that the FactSage database does not contain all the ternary compounds of the $K_2O-Al_2O_3-SiO_2$ system, it was necessary to add these data to FactSage from the thermodynamic values reported by Kim et al (2018). The chemical composition of the kaolin samples reported in Table 1, without the loss on ignition (LOI) value, was considered as base chemical composition and the K_2O content was evaluated for 0.1, 1.3, 2, and 3 wt % which cover the typical amounts of K_2O found in commercial kaolins (Castelein et al., 2001; Chandrasekhar and Ramaswamy, 2002; Fabbri et al., 2013). The formed compounds and their quantity during thermal treatment of kaolin clays were determined from 600 to 1600°C. The rheological behavior of the melt was determined at 1400, 1500, and 1600°C with the viscosity model contained in FactSage 7.3, which relates the viscosity with the structure of the melt by using the modified Quasichemical model (Bale et al., 2009). The system $Al_2O_3-SiO_2-K_2O-TiO_2-Fe_2O_3$ considered in the thermodynamic modeling contain as major components to the Al_2O_3 and SiO_2 components, these major oxide components together with Fe_2O_3 have been fully optimized and evaluated for binary and ternary systems at all compositions. In the present work, the amount of $TiO_2 + K_2O$ is less than 0.2% and 2.0% for Kaolin clay A and B, respectively; then, great accurate calculations can be obtained since the main components of the samples are the oxides which have been extensively evaluated.

3. Results and discussion

3.1. Raw materials

The chemical and mineralogical composition, the specific surface area, and the average particle size of the kaolin clay samples are shown in Table 1.

Table 1. Characteristics of the kaolin raw materials composition (mass %)

	Kaolin clay A		Kaolin clay B	
	Chemical	Mineralogical	Chemical	Mineralogical
SiO_2	46.65	Kaolinite = 21 (\pm 2)	46.38	Kaolinite = 46 (\pm 3)
Al_2O_3	44.27	Quartz = 7 (\pm 1)	36.86	Quartz = 12 (\pm 2)
Fe_2O_3	0.14	Cristobalite = 26 (\pm 3)	0.81	Cristobalite = 4 (\pm 2)
K_2O	0.1	Tridymite = 39 (\pm 2)	1.34	Tridymite = 24 (\pm 3)
TiO_2	0.09	Alunite = 7 (\pm 1)	0.66	Alunite = 14 (\pm 2)
LOI at 1000°C	8.75		13.95	
Average particle size (μm)	6.207		13.3	
Specific surface area ($m^2 \cdot g^{-1}$)	22.019		13.162	

The SiO_2 content is very similar for both samples. The Al_2O_3 content is higher for kaolin clay A and the impurity contents namely Fe_2O_3 , K_2O , and TiO_2 are much lower than Kaolin clay B. It is expected that the higher content of silica in both kaolin clays reduces plasticity as well the LOI (Schroeder et al., 2004; Peters, 1988). The amounts of K_2O and TiO_2 depend on illite/mica and anatase content. The mineralogical characterization is observed in Table 1, the quantification performed by the Rietveld method showed that kaolin clays A and B contain 21 and 46 wt % of kaolinite, respectively. The silica polymorphs were also detected where the tridymite amount is higher than quartz and cristobalite in both samples. The presence of tridymite indicates a pervasive hydrothermal alteration properly of the Agua Blanca zone located in the sedimentary series of the "Sierra Madre Oriental". The kaolin raw materials also contain alunite, where the kaolin clay A shows the lowest amount. Based on the mineralogical composition, the kaolin clay B could be considered as a silica-rich kaolinitic clay while the kaolin clay A corresponds to a kaolinitic clay. In general, the chemical and mineralogical composition of both kaolin clay samples is in the range expected for the Agua Blanca zone (M. Garcia et al., 2015).

The kaolin samples were characterized by X-ray powder diffraction. The characterization results are shown in Fig. 1.

It is observed from Fig. 1a that the main component of the sample of kaolin clay A is the kaolinite (JCPDS file 96-900-9231), cristobalite (JCPDS file 96-900-9688), tridymite (JCPDS file 96-901-3394), and quartz (JCPDS file 96-900-9667); also, small amounts of alunite (JCPDS file 96-901-6103) and anatase (JCPDS file 96-900-8217) were also detected. Fig. 1b shows the XRD pattern of the sample of kaolin clay B. The diffractogram is mainly formed by kaolinite, the SiO₂ polymorphs, and the intensity of the diffracted peaks of alunite and anatase are increased. TiO₂ as anatase is a common mineral in kaolin deposits and it has been reported that the alunite compound KAl₃(SO₄)₂(OH)₆ may reach up to 10 wt % in Agua Blanca zone (M. Garcia et al., 2015). The presence of illite was not detected in the samples evaluated.

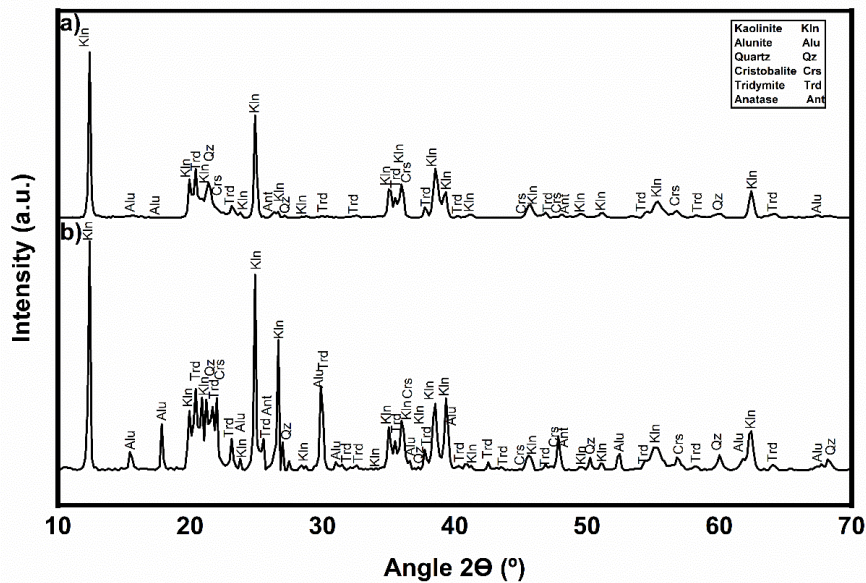


Fig. 1. XRD patterns of the samples of a) Kaolin clay A and b) Kaolin clay B as received at room temperature

The morphology and the qualitative chemical analysis by the EDS technique of the kaolin clay samples are shown in Figs. 2 and 3. A backscattered SEM image shows that the particles of the kaolin clay A sample reveal regular or elongated lamellar hexagonal flakes of kaolinite that are often grouped in booklets (Fig. 2a). Fig. 2b shows a similar particle array than Fig. 2a constituted by hexagonal kaolinite particles of varying sizes that are arranged in a face to face patterns. The flakes thickness is in the range from 10 to 20 nm for kaolin clay A and from 20 to 50 nm for kaolin clay B.

The EDS analysis of kaolin clay A (Fig. 3a) shows that the Al, Si, and O are the main elements homogeneously distributed in the particles. According to the XRD results, these particles correspond mainly to kaolinite and the silica polymorphs. Potassium, sulfur, and titanium are also observed and evidence the presence of alunite and rutile. Fig. 3b shows the microanalysis results in the sample of

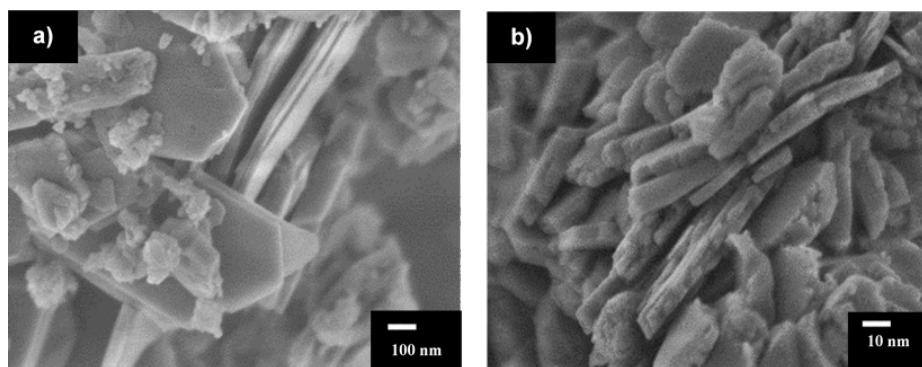


Fig. 2. SEM image of the kaolin raw material for (a) Kaolin clay A and, (b) Kaolin clay B

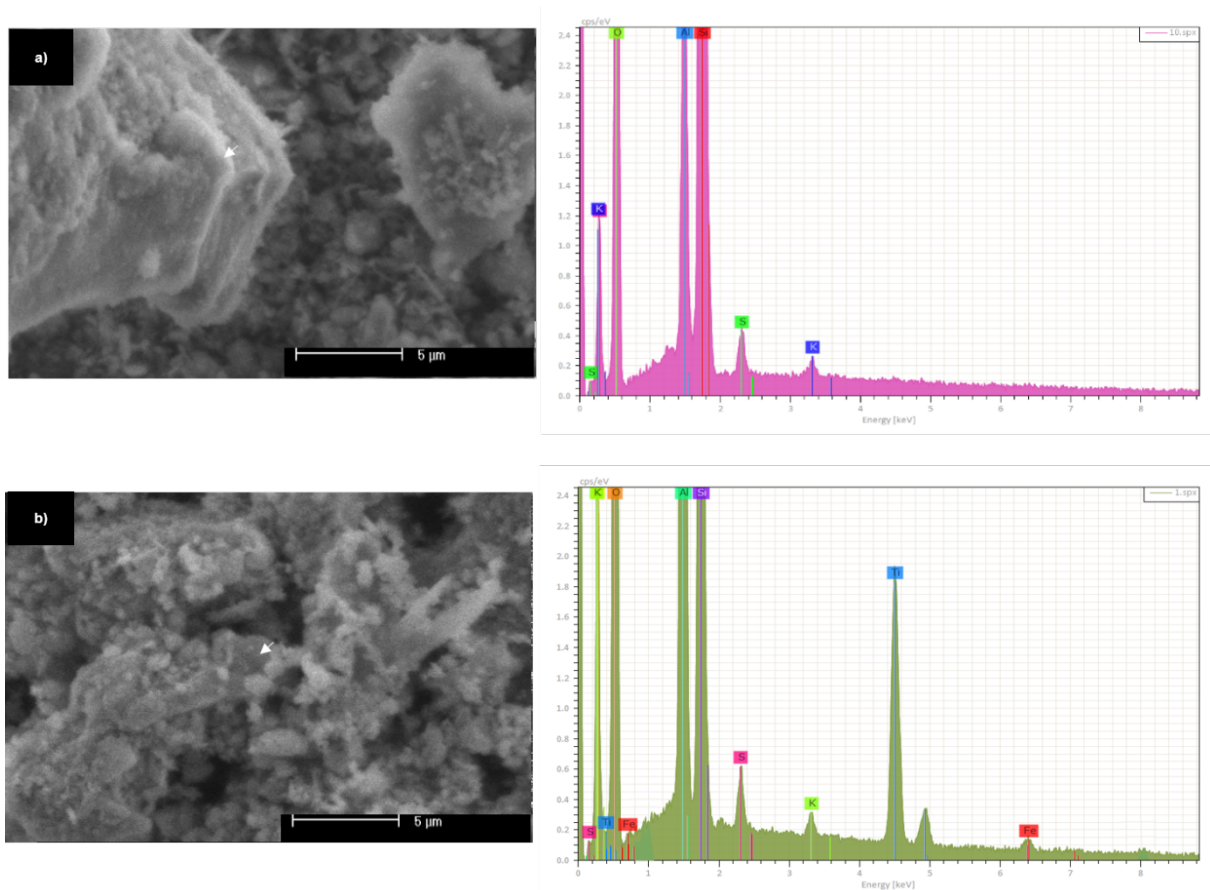


Fig. 3. SEM-EDS images of the kaolin clay samples analyzed for (a) Kaolin clay A and, (b) Kaolin clay B

kaolin clay B, it is observed the presence of high amounts of Al, Si, and O included in compositions of the kaolinite and the silica polymorphs. Impurities of K, Ti, and S are also detected in the kaolin clay B sample but in higher amounts than kaolin clay A. These elements correspond to the alunite and rutile minerals, as it was observed by the X-ray powder diffraction technique. Small amounts of iron were observed in the kaolin clay B sample and it could be forming hematite.

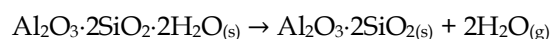
3.2. Thermal treatment

The thermal behavior of the two kaolin clay samples is shown in Fig. 4. The TGA curves show a weight reduction of around 9 wt % and 14 wt %, for kaolin clay A and B, respectively. The global mass loss for both kaolin clays is in agreement with the results reported in Table 1.

A slight reduction in weight occurs due to the loss of water and the burning of organic materials to low temperatures (Mohsen and El-maghraby, 2010). In the range from 500 to 600°C, de-hydroxylation of kaolin minerals to amorphous form occurs and it is associated with a weight loss of 13.76 % to pure kaolinite (Tironi et al., 2012). The decomposition of kaolin occurs in the range from 700 to 800°C, where the alunite ($KAl(SO_4)_2$) decomposition to K_2SO_4 , Al_2O_3 , and SO_3 occurs at around 710°C (Kakali et al., 2001; Küçük and Gülaboğlu, 2002). The de-hydroxylation rate of kaolinite can vary depending on mineralogical, chemical, and physical characteristics of the treated kaolin clay.

The results from DSC curves show that the first event is a broad endothermic peak at around 500 - 600°C for both kaolin clay samples, corresponding to the de-hydroxylation of kaolinite, the center of the endothermic peaks appears at around 550 and 560°C for the kaolin clays A and B, respectively.

During the calcination, dehydroxylation of kaolinite produces an amorphous phase (metakaolinite) according to the following reaction (Salvador, 1995):



A second event appears at 1000°C where the exothermic peak is assigned to the metakaolinite (and

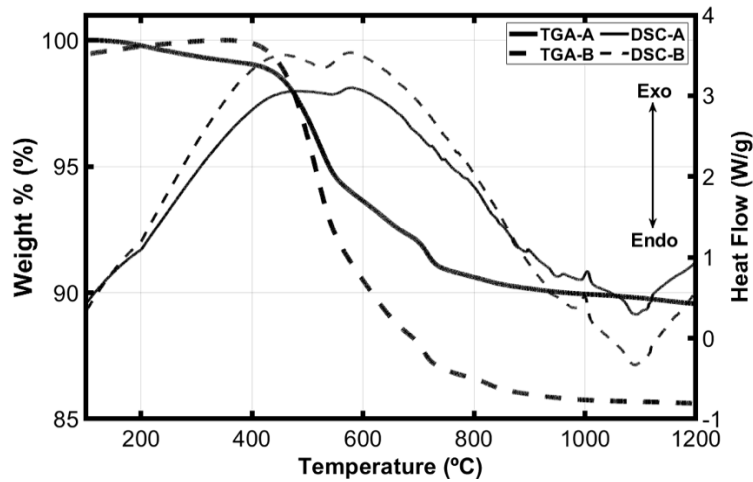


Fig. 4. TGA-DSC curves of the two kaolin clay samples

amorphous) transformation to spinel and amorphous silica. At 1100°C mullite develops largely highly crystalline cristobalite due to the spinel phase nucleation.

The kaolin clay samples were calcined in the range from 500 to 1100°C and then characterized by X-ray powder diffraction to determine the compound transformations as thermal treatment is applied. The XRD of the kaolin clay samples as received and heat-treated at 500, 950, and 1100°C are shown in Fig. 5. As it is observed, the kaolin clay samples content kaolinite, alunite, the silica polymorphs, and

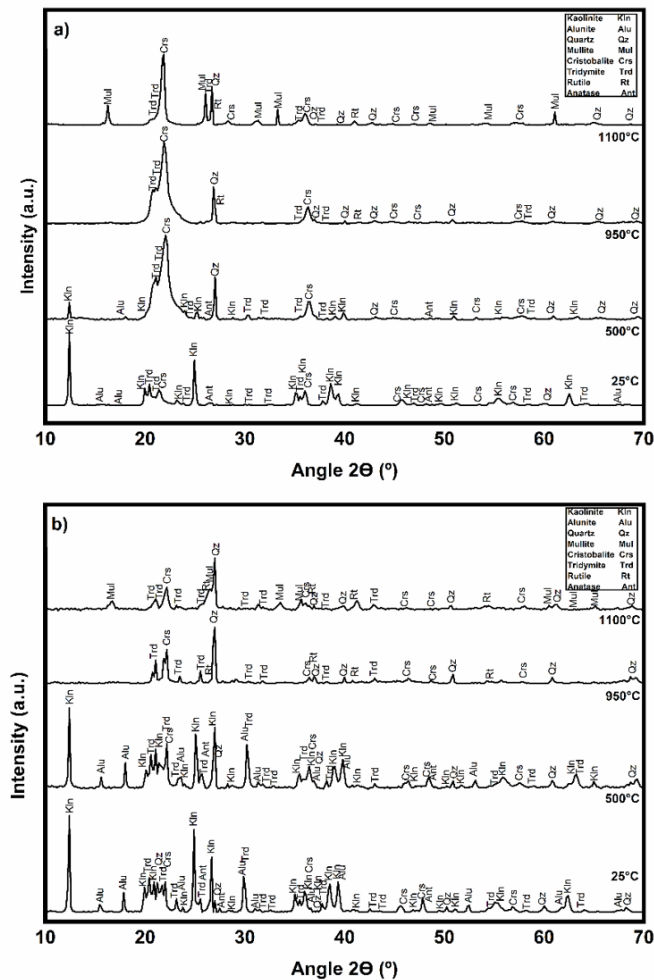


Fig. 5. XRD patterns of the samples of a) Kaolin clay A and b) Kaolin clay B as received, and heat-treated to 500°C, 950°C, and 1100°C

a small amount of anatase. The basic minerals that are identified at room temperature remain at 500°C; however, it was observed a lower intensity of the kaolinite peaks in both kaolin clay samples. As temperature increases at 950°C, the kaolinite and alunite peaks disappear and only the SiO₂ polymorphs are observed together with small amounts of rutile. The heat-treated samples at 1100°C show the mullite formation and the silica presence as cristobalite, tridymite, and quartz for both kaolin clays. Small amounts of rutile are also presented at high temperatures for both kaolin clay samples.

Table 2 shows the quantification performed by the Rietveld method for the kaolin clay samples heat treated at 1100°C. The results of Table 2 show that the amount of mullite and tridymite are greater for kaolin clay A than kaolin clay B while the amount of quartz is lower in kaolin clay A than kaolin clay B sample. Cristobalite is almost constant for both kaolin clay samples.

Table 2. Mineralogical composition (global mass %) of the kaolin clay samples heat treated at 1100°C

Mineral	Kaolin clay A	Kaolin clay B
Quartz	17 (± 2)	35 (± 3)
Cristobalite	24 (± 3)	23 (± 2)
Tridymite	18 (± 2)	9 (± 2)
Mullite	41 (± 3)	33 (± 2)

3.3. Thermodynamic modeling

The calculated mineralogical composition in wt. % obtained by FactSage 7.3 (Bale et al., 2002) considering the chemical composition of the kaolin clay samples to different temperatures and K₂O contents are shown in the stability phase diagrams of Figs. 6 and 7 for kaolin clay A and B, respectively.

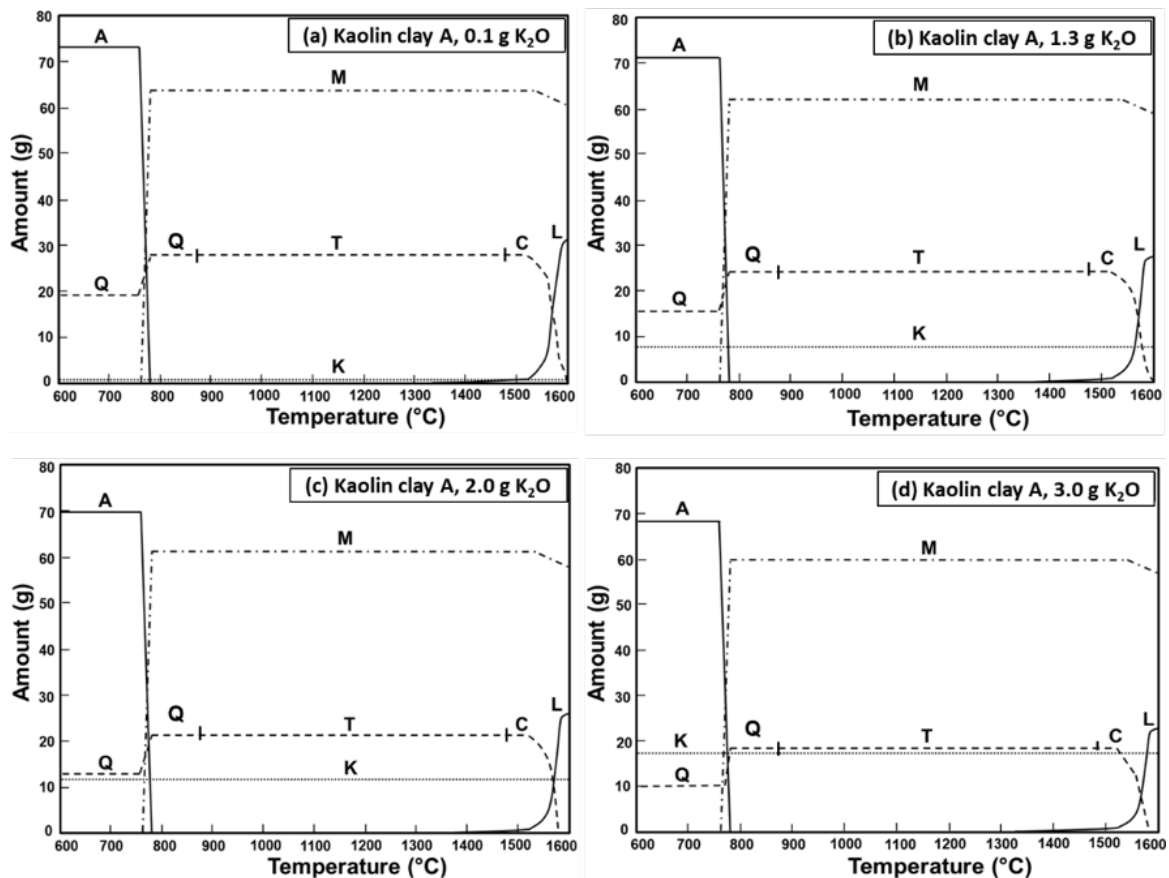


Fig. 6. Mineralogical composition (wt. %) formed in terms of temperature and K₂O content for the sample of kaolin clay A. A-Andalusite (Al₂O₃ · SiO₂); K-Potash feldspar (K₂O · Al₂O₃ · 6SiO₂); M-Mullite (3Al₂O₃ · 2SiO₂); Q-Quartz (SiO₂); T-Tridymite (SiO₂); C-Cristobalite (SiO₂); L-Liquid

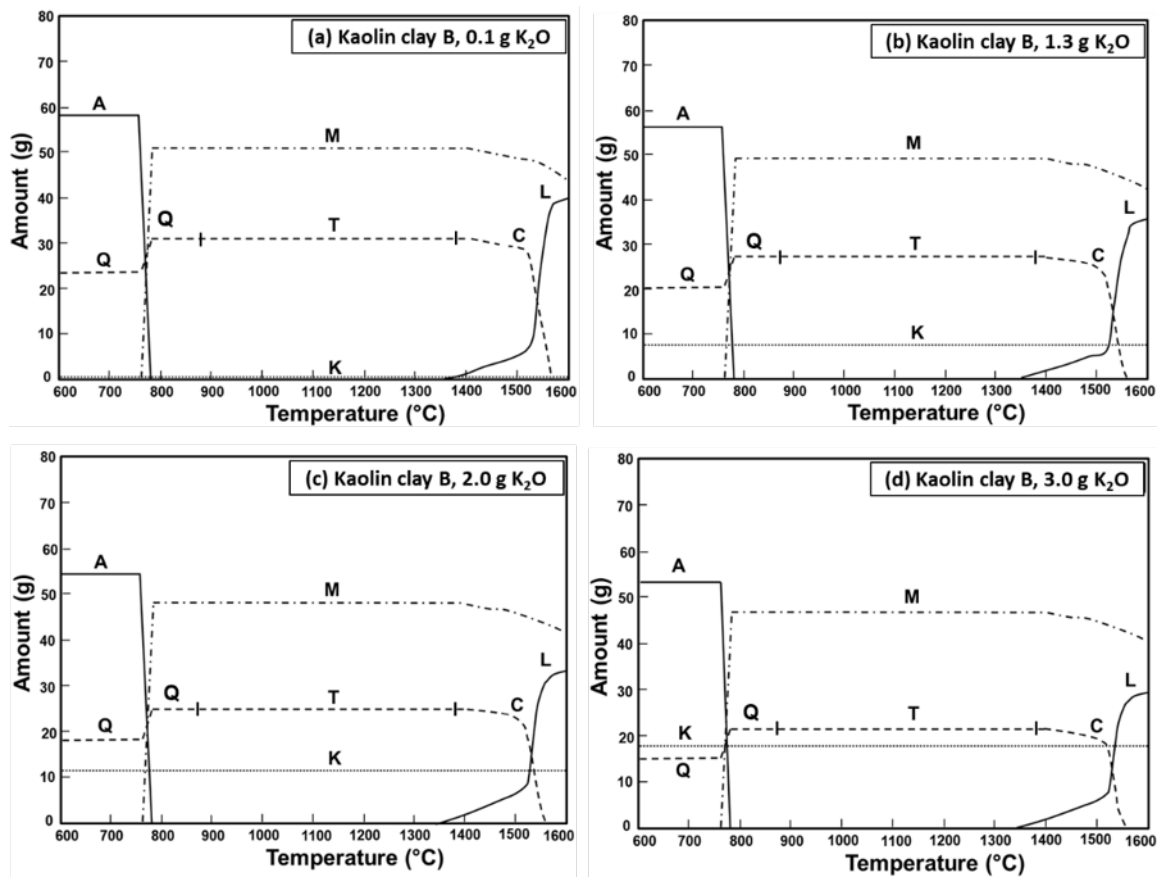


Fig. 7. Mineralogical composition (wt.%) formed in terms of temperature and K_2O content for the sample of kaolin clay B. A-Andalusite ($Al_2O_3 \cdot SiO_2$); K-Potash feldspar ($K_2O \cdot Al_2O_3 \cdot 6SiO_2$); M-Mullite ($3Al_2O_3 \cdot 2SiO_2$); Q-Quartz (SiO_2); T-Tridymite (SiO_2); C-Cristobalite (SiO_2); L-Liquid

The main compounds obtained at $600^\circ C$ are andalusite ($Al_2O_3 \cdot SiO_2$), potash feldspar ($K_2O \cdot Al_2O_3 \cdot 6SiO_2$) and quartz (SiO_2) for both kaolin clay samples and the whole K_2O additions. Small amounts of hematite (Fe_2O_3) and rutile (TiO_2) were also obtained but they are not shown in Figs. 6 and 7. Andalusite and quartz are the main compounds but their amount diminished when the K_2O content is increased. As expected, when the K_2O content is increased, the potash feldspar phase is increased. When the temperature is increased at about $780^\circ C$, andalusite is not presented, and mullite ($3Al_2O_3 \cdot 2SiO_2$) is formed. The stability region of the andalusite phase is in agreement with the experimental determination carried out by M. Holdaway (1971) where andalusite is stable in the range from 200 to $770^\circ C$ at 1 atm, and the results reported by R. A. Robie et al. (1979) and S. Saxena et al. (1993). Quartz is transformed into tridymite at $867^\circ C$. It is observed that above $780^\circ C$ mullite is the main compound followed by quartz and potash feldspar. The amount of mullite formed in kaolin clay A is higher than that of kaolin clay B because the former contains a higher initial amount of Al_2O_3 . As the K_2O content is increased, the amount of mullite and quartz compounds is decreased while the potash feldspar compound is increased. When the temperature is increased to about $1000^\circ C$, the hematite compound is not formed, and the software predicts that the iron oxide is combined with titanium to form the ferric-pseudobrookite (Fe_2O_5Ti) compound with a small decrease of rutile compound. From $780^\circ C$ to about $1450^\circ C$ for kaolin clay A and $1350^\circ C$ for kaolin clay B, the amounts and compounds formed, mullite, potash feldspar and silica (quartz or tridymite) remain constant. Figs. 6 and 7 also show that tridymite is transformed into cristobalite at $1465^\circ C$. The software prediction is in agreement with the results reported in Table 2 for the mullite, tridymite, quartz, and cristobalite compounds formation at $1100^\circ C$. However, the andalusite and potash feldspar compounds were not detected by XRD due to thermal treatment conditions where longer times are required to reach thermodynamic equilibrium.

The initial melting temperatures for the kaolin clay samples A and B are of 1450 and $1350^\circ C$, respectively and a bigger liquid zone is formed in kaolin clay sample B due to lower Al_2O_3 content. It is

observed from Figs. 6 and 7 that liquid regions still contain the solid compounds cristobalite and potash feldspar which will be consumed as the temperature is increased. The $\text{SiO}_2\text{-Al}_2\text{O}_3\text{-K}_2\text{O}$ phase equilibrium diagram (Schairer and Bowen, 1955) shows that it's possible to form potash feldspar to high K_2O contents and low Al_2O_3 contents. G. Lecomte et al (2004) studied the low alumina region of the $\text{SiO}_2\text{-Al}_2\text{O}_3\text{-K}_2\text{O}$ ternary system where no experimental data are available by thermodynamic analysis and experimental quenching test. The region analyzed comprise the lines connecting mullite with the ternary eutectic at 985°C and mullite with the peritectic point at 1140°C . The chemical composition of the kaolin clays analyzed is close to the zone studied by G. Lecomte et al (2004) and are in agreement with the existence of a large subliquidus immiscibility zone in the mullite-rich region and validate the existence of two horizontal lines at 985 and 1140°C , below which mullite, potash feldspar, and silica crystallize.

Figs. 8 and 9 show the effect of adding K_2O to the chemical base composition at 1100°C for the sample of kaolin clays A and B, respectively. Under these conditions, three main phases were formed, mullite, tridymite, and potash feldspar, also minor compounds like ferric-pseudobrookite and rutile were formed and they are not represented in these figures. It is observed, that the increase of the K_2O additions to the kaolin clays, decrease the amounts of mullite and tridymite, while the potash feldspar compound is increased. Most of the reported works point out that the potassium addition to kaolinite allows obtaining during heating mainly mullite and inhibition of SiO_2 as cristobalite or tridymite according to the temperature of the heat treatment (Aras, 2004; Li et al., 2009; Yamuna et al., 2002). The thermodynamic results agree with the results reported (Aras, 2004; Li et al., 2009; Yamuna et al., 2002).

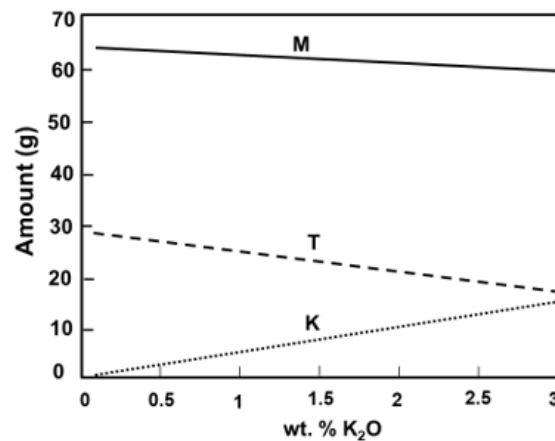


Fig. 8. Effect of the K_2O addition on the formation of the mineralogical species for the sample of kaolin clay A at 1100°C . K-Potash feldspar ($\text{K}_2\text{O}\cdot\text{Al}_2\text{O}_3\cdot 6\text{SiO}_2$); M-Mullite ($3\text{Al}_2\text{O}_3\cdot 2\text{SiO}_2$); T-Tridymite (SiO_2)

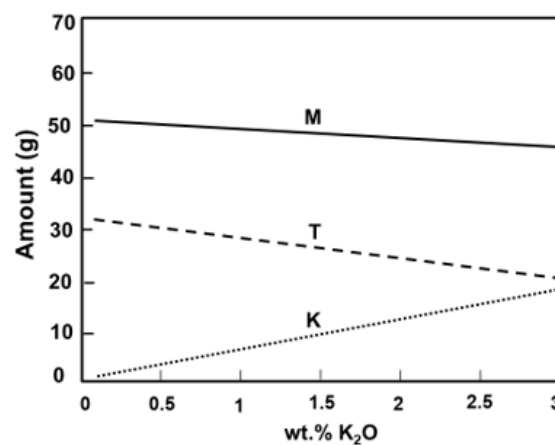


Fig. 9. Effect of the K_2O addition on the formation of the mineralogical species for the sample of kaolin clay B at 1100°C . K-Potash feldspar ($\text{K}_2\text{O}\cdot\text{Al}_2\text{O}_3\cdot 6\text{SiO}_2$); M-Mullite ($3\text{Al}_2\text{O}_3\cdot 2\text{SiO}_2$); T-Tridymite (SiO_2)

From Figs. 8 and 9 it is observed that the potash feldspar is formed as the mullite and tridymite compounds are consumed when the K_2O is increased. The kaolin clay samples A and B contain 64, 29, 0.2 wt % and 49, 28, and 8 wt % of mullite, tridymite, and potash feldspar, respectively. The results are in agreement with the mullite and tridymite formation by DRX; however, the potash feldspar was not detected due to the mineralogical composition of the kaolin clay samples and the thermal treatment applied; therefore, controlled quenching trials, pure compounds among other experimental parameters are required to reach thermodynamic equilibrium.

In contrast to the alkaline earth aluminosilicate systems, the alkali aluminosilicate systems exhibit more complicated viscosity behavior (Wu, 2015). The viscosity model considered the associated compounds in the system $SiO_2-Al_2O_3-K_2O$ (Kim, 2018). The rheological properties of the kaolin clays were evaluated by the viscosity determination at 1400, 1500, and 1600°C as can be observed in Figs. 10 and 11 for the kaolin clay A and B, respectively. It is important to note that the viscosity model contained in Factsage was developed for a fully liquid slag system.

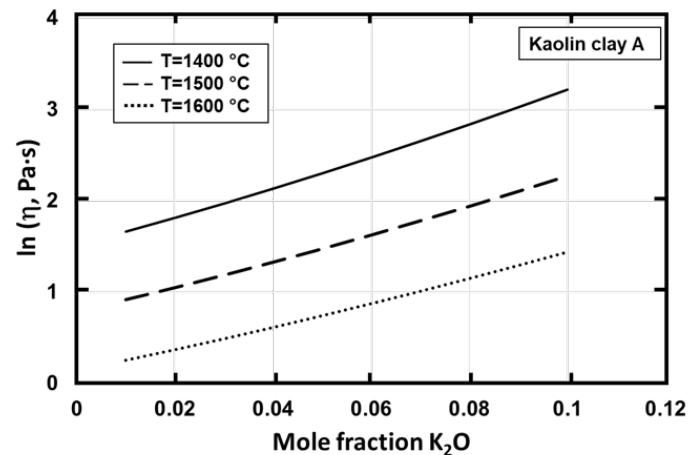


Fig. 10. Effect of the K_2O addition on the viscosity ($\ln [\eta, Pa \cdot s]$) for kaolin clay A at 1400, 1500, and 1600°C

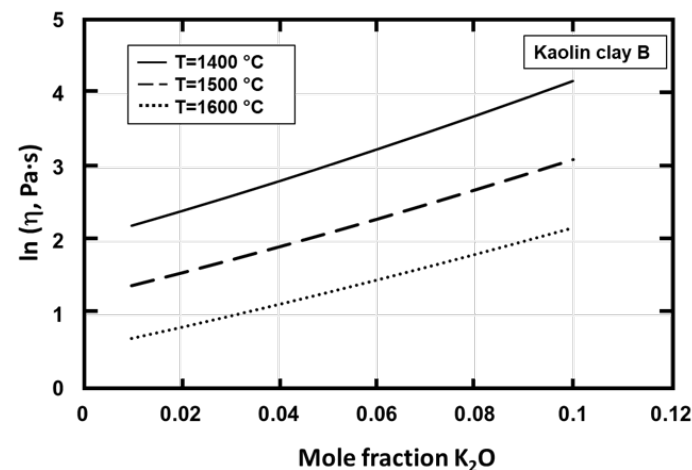


Fig. 11. Effect of the K_2O addition on the viscosity ($\ln [\eta, Pa \cdot s]$) for kaolin clay B at 1400, 1500, and 1600°C

The viscosity is increased as the K_2O is increased for both kaolin clays for the evaluated temperatures. As network former, the higher silica and alumina content in kaolin clay A allows obtaining a higher viscosity than kaolin clay B. As expected, the viscosity decreased when the temperature is increased. The presence of Na and K as oxides decrease the melting temperature also acting as fusing in kaolins (Schroeder et al., 2004) and decrease the viscosity of the calcium aluminosilicate melts (Kim et al., 2010; Zhang and Chou, 2012). However, the thermodynamic results show an increase of the melt viscosity for the low amounts of K_2O considered in both kaolin clays. This behavior is attributed to the $K_2O - AlO_4$ interaction. It has been reported (Higo et al., 2014) that the increase of viscosity with an increment in the K_2O content when K_2O/Al_2O_3 molar ratio lower than 0.7

but decreased when the K_2O content was K_2O/Al_2O_3 molar ratio higher than 0.9. For a higher K_2O/Al_2O_3 molar ratio, the non-bridging oxygens (NBOs) increased and the aluminosilicate network structure is depolymerized after the addition of K_2O . On the other hand, a lower K_2O/Al_2O_3 molar ratio increases the average bond strength of the aluminosilicate network.

Fig. 12 shows the viscosity determination compared with the results reported by G. Wu (2015) for the $SiO_2-Al_2O_3-K_2O$ ternary system and similar mole fraction SiO_2 . For these conditions, the viscosity is increased as the mole fraction K_2O is increased, and the results of kaolin clay B reasonably match with the results reported by G. Wu (2015). Despite the Al^{3+} cation plays the role of a network modifier, when Al^{3+} is charge-compensated by K^+ and forms the $KAlO_2$ quasi-tetrahedra, this compound is not capable of forming large network structures. For the $SiO_2-Al_2O_3-K_2O$ ternary system, the viscosity increase as the amount of K_2O is increased reaching a maximum value for the mole fraction $Al_2O_3/(Al_2O_3 + K_2O)$ at around 0.45 at $1400^\circ C$ and then, the viscosity decreases sharply (Wu, 2015). However, more experimental data are needed to better assess the model parameters for alkali aluminosilicate systems.

The chemical composition of kaolin clay A corresponds to the typical chemical composition of refractory clays referred as a medium alumina refractory, ranging from about 45 to over 70 wt % alumina content (Harbison-Walker, 1992), while the kaolin clay B could be used as a raw material for the manufacturing of fluxes used for steel refining whereas the viscosity of aluminosilicate plays a significant role in the steelmaking process (Zhang and Chou, 2012) and the results presented in Figs. 9 to 11 could be useful, especially for the scarcity of experimental data reported for the ternary $SiO_2-Al_2O_3-K_2O$ system evaluated.

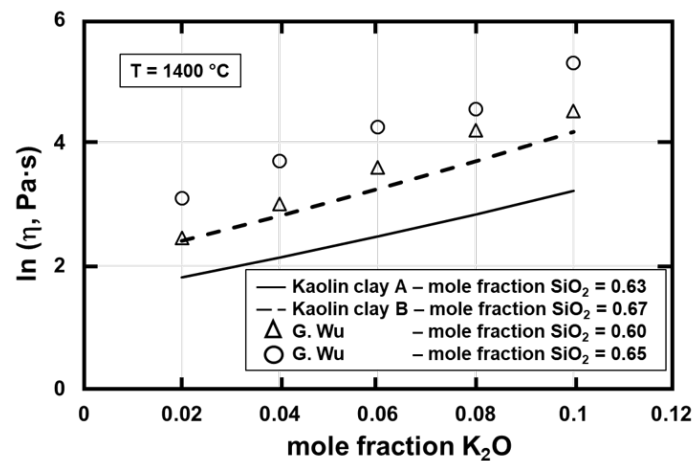


Fig. 12. Comparison between calculated data for viscosity in the system $SiO_2-Al_2O_3-K_2O$ at $1400^\circ C$

4. Conclusions

A thermodynamic analysis was carried out considering the chemical composition of two kaolin clay samples from Agua Blanca (Hidalgo-México) with the FactSage 7.3 software. The compound predicted by the software were determined to different K_2O contents (0.1 to 3 wt %) and temperatures (600 to $1600^\circ C$). The main mineralogical compounds predicted are andalusite ($Al_2O_3 \cdot SiO_2$), K-Potash feldspar ($K_2O \cdot Al_2O_3 \cdot 6SiO_2$), and the SiO_2 polymorphs (quartz, tridymite, and cristobalite) with small amounts of ferric-pseudobrookite (Fe_2O_5Ti), and rutile (TiO_2). The mullite and SiO_2 polymorphs are in agreement with the XRD results at $1100^\circ C$. The increase of the K_2O amount promotes a decrease in the mullite which could be detrimental for ceramic applications, also the tridymite decreased while the K-Potash feldspar was increased. The viscosity of the fused kaolin clays was evaluated at 1400, 1500, and $1600^\circ C$ where a liquid region was predicted, located at $1350^\circ C$ and $1450^\circ C$ for kaolin clay B and A, respectively. The viscosity of the melt was increased when the temperature was decreased and the K_2O content was increased from 1 to 10 mol %. Thereby, the viscosity of the melt increases due to a growth in the average bond strength of the aluminosilicate network for the low K_2O contents in the clay samples. As expected, kaolin clay A which contains the higher Al_2O_3 amount showed the highest mullite content and viscosity values than kaolin clay B. Alike SiO_2 content for both kaolin clays allows obtaining almost the same amount of tridymite during heating. The viscosity results could be used to understand the rheological

behavior of the melt, especially for ironmaking or steelmaking process where a fluid slag is required during the refining process and experimental viscosity data are not available due to the experimental difficulty to obtain viscosity data at high temperatures.

Acknowledgments

The authors wish to thank to the Institutions UAEH, CONACyT, SNI, CINVESTAV - Unidad Querétaro, Cooperativa La Cruz Azul S.C.L. Product Engineering Laboratory Department and Thermal Analysis laboratory at Materials Research Institute – UNAM Polymers Department. Besides, A.C.R, R.G.S.A., and J.A.R.S. wishes to thank COFAA and SIP-Instituto Politécnico Nacional for their permanent assistance to the Process Metallurgy Group at ESIQIE-Metallurgy and Materials Department.

References

- ARAS, A., 2004. *The change of phase composition in kaolinite- and illite-rich clay-based ceramic bodies*. Appl. Clay Sci. 24(3–4), 257–269.
- BALE, C. W., CHARTRAND, P., DECTEROV, S. A., ERIKSSON, G., HACK, K., BEN MAHFOUD R., MELANQON J., PELTON A.D. AND PETERSEN, S., 2009. *FactSage thermochemical software and databases - recent developments*. Calphad: Comput. Coupling of Phase Diagrams and Thermochem. 33(2), 295–311.
- BLOODWORTH, A. J., HIGHLEY, D. E., MITCHELL, C. J., 1993. *Industrial Minerals Laboratory Manual: Kaolin BGS Technical Report WG/93/1*. 2014.
- BULENS, M., DELMON, B., 1977. *The exothermic reaction of metakaolinite in the presence of mineralizers. Influence of crystallinity*. Clays Clay Miner. 25(4), 271–277.
- BALE C.W., CHARTRAND P., DEGTEROV S.A., ERIKSSON G., HACK K., MAHFOUD R. B., MELANQON J., PELTON A. D., PETERSEN S., 2002. *FactSage thermochemical software and databases*. Calphad. 26(2), 189–228.
- CARTER, C. B., NORTON, M. G., 2013. *Ceramic Materials: Science and Engineering*. Ceram. Mater. Sci. Eng. 1–766.
- CASTELEIN, O., SOULESTIN, B., BONNET, J. P., BLANCHART, P., 2001. *The influence of heating rate on the thermal behaviour and mullite formation from a kaolin raw material*. Ceram. Int. 27(5), 517–522.
- CHAKRABORTY, A. K., 2014. *Phase transformation of kaolinite clay*. Chapter 1, India, Springer.
- CHANDRASEKHAR, S., RAMASWAMY, S., 2002. *Influence of mineral impurities on the properties of kaolin and its thermally treated products*. Appl. Clay Sci. 21(3–4), 133–142.
- CHEARY, R.W., COELHO, A.A., 1992. *A fundamental parameters approach to X-ray line-profile fitting*, J. Appl. Cryst. 25, 109.
- DE PABLO-GALÁN, L., 1978. *The clay deposits of Mexico*. Proceedings of the VI Int. Clay Conf. 27, 475–486.
- FABBRI, B., GUALTIERI, S., LEONARDI, C., 2013. *Modifications induced by the thermal treatment of kaolin and determination of reactivity of metakaolin*. Appl. Clay Sci. 73(1), 2–10.
- GARCIA-VALLES, M., PI, T., ALFONSO, P., CANET, C., MARTÍNEZ, S., JIMÉNEZ-FRANCO, A., TARRAGO, M., HERNÁNDEZ-CRUZ, B., 2015. *Kaolin from Acoculco (Puebla, Mexico) as raw material: Mineralogical and thermal characterization*. Clay Miner. 50(3), 405–416.
- HIGO, T., SUKENAGA, S., KANEHASHI, K., SHIBATA, H., OSUGI, T., SAITO, N., NAKASHIMA, K., 2014. *Effect of potassium oxide addition on viscosity of calcium aluminosilicate melts at 1 673-1 873 K*. ISIJ Int. 54(9), 2039–2044.
- HOLDAWAY, M.J., 1971. *Stability of andalusite and the aluminum silicate phase diagram*. Am. J. Sci. 271, 97–131.
- H.-W. Refractory Company, 1992. *Modern refractory practice*. Pittsburgh: Harbison-Walker Refractories Company.
- JOHNSON, S. M., PASK, J. A., MOYA, J. S., 1982. *Influence of Impurities on High-Temperature Reactions of Kaolinite*. J. Am. Ceram. Soc. 65(1), 31–35.
- KAKALI, G., PERRAKI, T., TSIVILIS, S., BADOGIANNIS, E., 2001. *Thermal treatment of kaolin: the effect of mineralogy on the pozzolanic activity*. Appl. Clay Sci. 20, 73–80.
- KIM, D-G., KOMAR, B., JUNG, I-H., 2018. *Thermodynamic optimization of the K₂O-Al₂O₃-SiO₂ system*. Ceram Int., 44(14), 16712-16724.
- KIM, W. H., SOHN, I., MIN, D. J., 2010. *A study on the viscous behaviour with K₂O additions in the CaO-SiO₂-Al₂O₃-MgO-K₂O quinary slag system*. Steel Res. Int. 81(9), 735–741.
- KISELEVA, I. A., OROGODOVA, L. P., KRUPSKAYA, V. V., MELCHAKOVA, L. V., VIGASINA, M. F., LUSE, I., 2011. *Thermodynamics of the kaolinite-group minerals*. Geochemistry Int. 49(8), 793–801.
- LECOMTE, G. L., BONNET, J. P., BLANCHART, P., 2007. *A study of the influence of muscovite on the thermal transformations of kaolinite from room temperature up to 1100°C*. J. Mater. Sci. 42, 8745-8752.

- LECOMTE, G. L., BONNET, J. P., BLANCHART, P., 2011. *Investigation of the sintering mechanisms of kaolin-muscovite*, Appl. Clay Sci., 51, 445-451.
- LECOMTE, G. L., PATEYRON, B., BLANCHART, P., 2004. *Experimental study and simulation of a vertical section mullite-ternary eutectic (985°C) in the SiO₂-Al₂O₃-K₂O system*. Mat. Res. Bulletin. 39, 1469-1978.
- LI, J., LIN, H., LI, J., & WU, J., 2009. *Effects of different potassium salts on the formation of mullite as the only crystal phase in kaolinite*. J. Eur. Ceram. Soc. 29(14), 2929-2936.
- KÜBÜK, A., GÜLABOĞLU, M. Ş., 2002. *Thermal decomposition of şaphane alunite ore*, Ind. Eng. Chem. Res. 41(24), 6028-6032.
- MICHOT, A., SMITH, D. S., DEGOT, S., GAULT, C., 2008. *Thermal conductivity and specific heat of kaolinite: Evolution with thermal treatment*. J. Eur. Ceram. Soc. 28(14), 2639-2644.
- MOHSEN, Q., EL-MAGHRABY, A., 2010. *Characterization and assessment of Saudi clays raw material at different area*. Arab. J. Chem. 3(4), 271-277.
- MORENO-TOVAR, R., PÉREZ-MORENO, F., ARENAS-FLORES, A., ROMERO-GUERRERO, L. M., 2014. *Thermal behavior, chemical, mineralogical and optical characterization of clays (kaolin) for industrial use as refractory material*. Adv. Mater. Res. 976(11), 174-178.
- PETERS, J., 1988. *Determination of undrained shear strength of low plasticity clays*. Proc. Symp. Adv. Triaxial Test. Soil Rock. 460-474.
- POTTS, P. J., 2003. *Handbook of rock analysis*. Science.
- ROBIE, R.A., HEMINGWAY, B.S., FISHER, J.R., 1979. *Thermodynamic properties of minerals and related substances at 298.15 K and 1 bar (10⁵ Pascals) pressure and at higher temperatures*, U.S. Geological Survey Bulletin, reprinted.
- SALVADOR, S., 1995. *Pozzolanic properties of flash-calcined kaolinite: a comparative study with soak calcined products*, Cement and Concrete Res., 25, 102-112.
- SAXENA, S.K., CHATTERJEE, N., FEI, Y., SHEN, G., 1993. *Thermodynamic data on oxides and silicates*. Berlin. Springer-Verlag.
- SCHAIRER, J. F., BOWEN, N. L. 1955. *The system K₂O-Al₂O₃-SiO₂*. Am. J. Sci. 253(12), 681-746.
- SCHROEDER, P. A., PRUETT, R. J., MELEAR, N. D. 2004. *Crystal-chemical changes in an oxidative weathering front in a Georgia kaolin deposit*. Clays Clay Miner. 52(2), 211-220.
- TIRONI, A., TREZZA, M.A., IRASSAR, E.F., SCIAN, A.N., 2012. *Thermal treatment of kaolin: effect on the pozzolanic activity*. Proc. Mater. Sci. 1, 343-350.
- WU, G. 2015. *Modelling and Experimental Validation of the Viscosity of Liquid Phases in Oxide Systems Relevant to Fuel Slags*. Universitätsbibliothek der RWTH Aachen.
- YAMUNA, A., DEVANARAYANAN, S., LALITHAMBIKA, M., 2002. *Phase-pure mullite from Kaolinite*. J. Am. Ceram. Soc. 85(6), 1409-1413.
- ZEGEYE, A., YAHAYA, S., FIALIPS, C. I., WHITE, M. L., GRAY, N. D., MANNING, D. A. C., 2013. *Refinement of industrial kaolin by microbial removal of iron-bearing impurities*. Appl. Clay Sci. 86, 47-53.
- ZHANG, G. H., CHOU, K. C., 2012. *Measuring and modeling viscosity of CaO-Al₂O₃-SiO₂(-K₂O) melt*. Metall. Mater. Trans. B: Process Metall. Mater. Process. Sci. 43(4), 841-848.